© 2021. Published by The Company of Biologists Ltd | Development (2021) 148, dev199825. doi:10.1242/dev.199825

RESEARCH ARTICLE

Avian ceca are indispensable for hindgut enteric nervous system development

Nandor Nagy[1,*,‡], Tamas Kovacs[1,*], Rhian Stavely[2], Viktoria Halasy[1], Adam Soos[1], Emoke Szocs[1], Ryo Hotta[2], Hannah Graham[2] and Allan M. Goldstein[2,‡]

ABSTRACT

The enteric nervous system (ENS), which is derived from enteric neural crest cells (ENCCs), represents the neuronal innervation of the intestine. Compromised ENCC migration can lead to Hirschsprung disease, which is characterized by an aganglionic distal bowel. During the craniocaudal migration of ENCCs along the gut, we find that their proliferation is greatest as the ENCC wavefront passes through the ceca, a pair of pouches at the midgut-hindgut junction in avian intestine. Removal of the ceca leads to hindgut aganglionosis, suggesting that they are required for ENS development. Comparative transcriptome profiling of the cecal buds compared with the interceca region shows that the non-canonical Wnt signaling pathway is preferentially expressed within the ceca. Specifically, WNT11 is highly expressed, as confirmed by RNA *in situ* hybridization, leading us to hypothesize that cecal expression of WNT11 is important for ENCC colonization of the hindgut. Organ cultures using embryonic day 6 avian intestine show that WNT11 inhibits enteric neuronal differentiation. These results reveal an essential role for the ceca during hindgut ENS formation and highlight an important function for non-canonical Wnt signaling in regulating ENCC differentiation.

KEY WORDS: Enteric nervous system, Ceca, Hindgut, Neural crest cells, Wnt11, Hirschsprung disease

INTRODUCTION

Development of the enteric nervous system (ENS) relies on carefully orchestrated interactions between enteric neural crest-derived cells (ENCCs) and their mesenchymal microenvironment as they proliferate, migrate, differentiate and pattern within the gastrointestinal tract to form a functional network of enteric neurons and glial cells. The ENS arises primarily from the craniocaudal migration of vagal neural crest-derived cells. These cells migrate from the dorsal part of the neural tube, adjacent to somites 1-7, and enter the chick foregut at embryonic day (E) 2.5, reaching the stomach at E4.5 and the midgut-hindgut junction at E5.5, passing through the ceca at E6.5 and reaching the distal end of the hindgut at E8 (Yntema and Hammond, 1954; Le Douarin and Teillet, 1973; Allan and Newgreen, 1980; Nagy et al., 2012). Additional contributions to the hindgut region come from sacral crest-derived ENCCs and Schwann cell precursors (Burns and Le Douarin, 1998; Nagy et al., 2007; Uesaka et al., 2015; Nagy and Goldstein, 2017). The most common developmental enteric neuropathy is Hirschsprung disease (HSCR), a congenital condition affecting 1 in 5000 newborns and characterized by the absence of enteric ganglia along variable lengths of distal intestine (Goldstein et al., 2016). Despite the presence of ENCC-associated mutations in HSCR, however, ENCCs colonize most of the intestine, with aganglionosis limited to the colon in >90% of cases, suggesting something potentially unique about the process of hindgut ENCC colonization (Amiel et al., 2008). The prevailing hypothesis for the pathogenesis of HSCR implicates deficiencies in ENCC proliferation or premature neuronal differentiation leading to insufficient numbers of ENCC progenitors completing the craniocaudal migration from foregut to rectum. However, why the cells can colonize nearly the entire gastrointestinal tract and only display migratory arrest in the colorectum is unknown and led us to hypothesize that ENCCs receive specific molecular signals as they cross from midgut to hindgut and that abnormalities in this region contribute to the etiology of HSCR.

The junction of the small and large intestine is marked by the cecum in mammals and by paired ceca in avians. This structure has been proposed to have an important role in hindgut ENS formation. For example, expression of GDNF and EDN3, ligands in key pathways implicated in HSCR pathogenesis, are spatially and temporally restricted to the cecal region in both mouse (Leibl et al., 1999; Young et al., 2001) and chick (Nagy and Goldstein, 2006a) intestine just prior to the arrival of ENCCs. In mice, EDN3-EDNRB signaling, which promotes ENCC proliferation and inhibits neuronal differentiation, is not required until the stage when ENCCs arrive in the cecum (Druckenbrod and Epstein, 2005; Shin et al., 1999; Woodward et al., 2003; Lee et al., 2003). Furthermore, the cecal environment has been shown to alter the migratory properties of ENCCs at the wavefront of migration to promote their colonization of the hindgut (Kruger et al., 2003; Nagy and Goldstein, 2006a). Here, we sought to understand the unique role of the ceca during hindgut ENS development and to determine how signaling pathways in the ceca impact migrating ENCCs to promote their migration into the colon.

RESULTS

ENCC migration through the chick distal intestine was evaluated by immunofluorescence at E5-E8. The migratory wavefront of ENCCs, which represents the migratory and undifferentiated neural crest-derived cells at or near the leading edge of migration, was present at the level of the distalmost midgut at E5 and marked by NCADH (CDH2) expression (Fig. 1A), which identifies all ENCCs (Nagy

[1]Department of Anatomy, Histology and Embryology, Faculty of Medicine, Semmelweis University, Budapest, 1094, Hungary. [2]Department of Pediatric Surgery, Pediatric Surgery Research Laboratories, Massachusetts General Hospital, Harvard Medical School, Boston, MA 02114, USA.
*These authors contributed equally to this work

‡Authors for correspondence (nagy.nandor@med.semmelweis-univ.hu; agoldstein@partners.org)

N.N., 0000-0002-6223-5214; R.H., 0000-0001-9890-8241; H.G., 0000-0002-2039-7717; A.M.G., 0000-0003-2106-847X

Handling Editor: François Guillemot
Received 25 May 2021; Accepted 22 October 2021

Development (2021) 148, dev199825. doi:10.1242/dev.199825

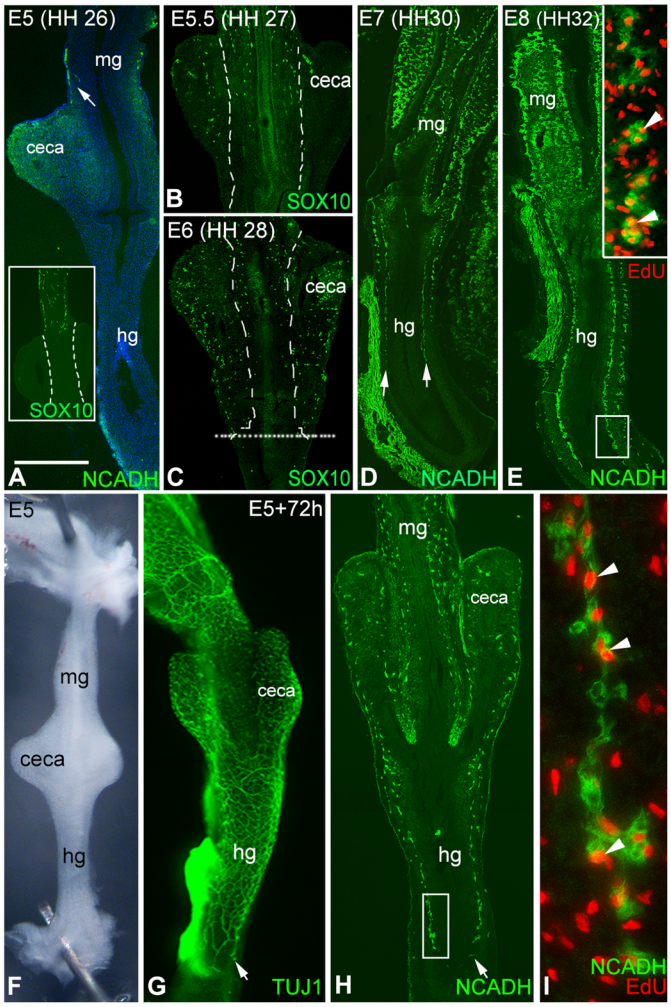

Fig. 1. ENS development in the ceca and hindgut *in vivo* and in organotypic culture. (A-E) Chick intestine was immunostained with N-cadherin (NCADH; A,D,E) and SOX10 (A inset,B,C) antibodies at E5-E8, showing progressive distal migration of ENCCs along the hindgut, with the leading edge of migration marked by arrows in A and D. The margin between ceca and interceca is marked by dashed lines. SOX10$^+$ ENCCs colonize the cecal region from E5.5 (B) to E6 (C). (F-I) Explanted E5 gut (F) becomes fully colonized by TUJ1$^+$ ENCCs after 72 h in culture (wholemount in G; longitudinal section in H; arrows mark migratory wavefront). NCADH$^+$ ENCCs proliferate at the wavefront (E, inset; boxed area in H is magnified in I). Arrowheads in I indicate proliferating cells. hg, hindgut; mg, midgut. Scale bar in A: 350 µm (A-C); 500 µm (D-G); 70 µm (inset in E); 400 µm (H); 40 µm (I).

et al., 2012). Because of non-specific NCADH staining in the cecal region, a SOX10 antibody was used as the cells traverse this region of the gut. At E5, SOX10-immunoreactive ENCCs were located just above the cecal buds (Fig. 1A, inset) and over the next 24 h migrated as a wavefront through the ceca and intercecal midgut (Fig. 1B) and into the proximal hindgut (Fig. 1C). At E7, the NCADH$^+$ wavefront was observed in the mid-hindgut (Fig. 1D), and by E8 it had reached the distal end (Fig. 1E). When E5 gut was explanted (Fig. 1F) and cultured in organotypic conditions for 3 days, ENCC colonization occured along a similar timeline (Fig. 1G,H). EdU incorporation confirmed the presence of proliferating ENCCs at the migratory wavefront (Fig. 1E,I).

Complete colonization of explanted E5 gut requires the few cells at the wavefront at E5 to undergo extensive cell proliferation. To determine whether the rate of proliferation varies along the length of the distal intestine, ENCC proliferation was quantified at various time points in cross-sections through the migratory wavefront by calculating the proportion of undifferentiated ENCCs that incorporate EdU (Fig. 2A). The undifferentiated wavefront cells were defined as those that express SOX10 but not HU (ELAVL4) (Fig. 2A′) or BFABP (FABP7) (Fig. 2A″). Measurements were performed at E5 (wavefront in distalmost midgut), E6 (wavefront in cecal region, with separate quantification of ENCC proliferation in the cecal buds and in the intercecal mesenchyme), E7 (wavefront in mid-hindgut) and E8 (colonization complete), with nine guts used per stage. The results, shown in Fig. 2B, reveal that wavefront ENCCs are most proliferative as they migrate through the cecal buds at E6, when the wavefront is located there, and this is significantly higher than in the wavefront when it is at the distal midgut (E5) or hindgut (E7). Although ENCC proliferation was higher in the ceca than in the interceca, this did not reach statistical significance.

The results above suggest an important role for the cecal region in hindgut ENS development. To test this, cecal buds were removed from E5 intestine, just prior to the arrival of migrating ENCCs (Fig. 3A,B) and the guts cultured for 3 days. Staining with TUJ1 (TUBB3) and NCADH showed ENCCs only extending to the proximal hindgut, with the remainder of the hindgut remaining aganglionic (Fig. 3C). Interestingly, the distalmost ENCCs formed large aggregates of cells with markedly reduced cell proliferation (Fig. 3D) compared with control (Fig. 1I), and this difference was statistically significant (Fig. 3G). The ENCC aggregates were highly differentiated and expressed nNOS (NOS1) (Fig. 3E), which marks a subset of terminally differentiated enteric neurons. No ENCC apoptosis was detected by caspase-3 staining (Fig. 3F). These results confirmed that the ceca are required for hindgut ENS formation. To explore this further, we removed the ceca at E6 and replaced them with new ceca harvested from age-matched green fluorescent protein (GFP)-expressing chick embryos (Fig. 4A). After 72 h in culture, GFP-expressing cells were seen migrating distally into the hindgut (Fig. 4B,C). These cells co-expressed NCADH (Fig. 4D,E), confirming that the GFP$^+$ cells migrating from the ceca represent ENCCs. Importantly, all the NCADH$^+$ cells in the hindgut co-expressed GFP$^+$ (Fig. 4E), suggesting that the hindgut ENS in these chimeric guts is entirely derived from ceca-derived ENCCs. There appeared to be no contribution from the ENS of the host gut, even though cells would have been able to migrate through the intercecal mesenchyme, which already contains ENCCs at E6 (Fig. 1C). This observation was further strengthened by DiI injection into the cecal buds at E5.5 (Fig. 5A). After 72 h, DiI-labeled cells were observed to have migrated into the hindgut (Fig. 5B,C) and co-expressed NCADH (Fig. 5D). Based on quantification under high-power magnification, we found that 31% of NCADH$^+$ ENCCs in the hindgut contained DiI crystals after cecal injection. In contrast, following injection of DiI into the intercecal region (Fig. 5E), no DiI-labeled cells were seen in the hindgut (Fig. 5F-H).

To identify the potential mechanisms of the cecal contribution to hindgut ENCC colonization, the molecular environment of the cecal and intercecal regions was characterized by RNA sequencing (RNA-seq). The ceca and interceca were carefully dissected at E5, immediately prior to ENCC colonization, to determine regional transcriptional differences (Fig. 6A). E5 was chosen as it is the earliest stage at which the ceca can be isolated because there are no cecal buds prior to this stage. E5 also allowed us to focus on the cecal microenvironment, without ENCC contamination, as at this stage it is being primed for ENCC arrival. Distinct changes in gene

Development (2021) 148, dev199825. doi:10.1242/dev.199825

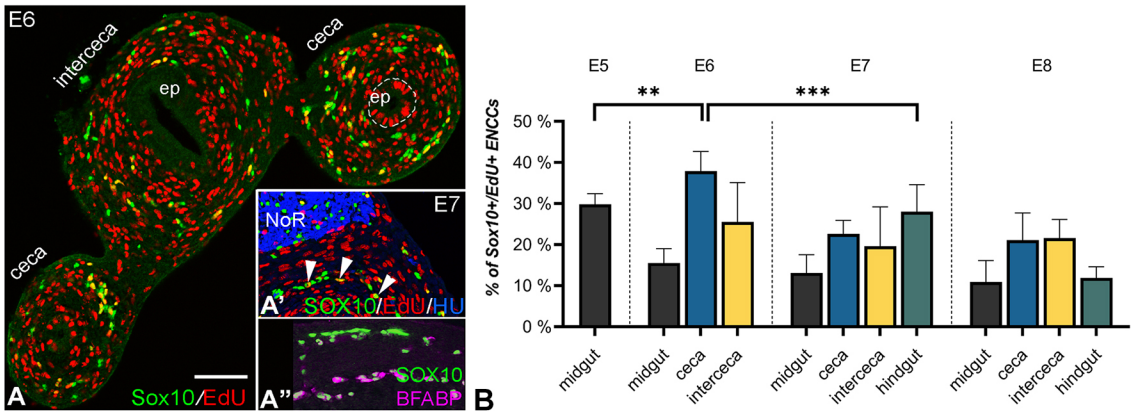

Fig. 2. ENCC proliferation is highest as the wavefront migrates through the cecal region. (A) Cross-section through the ceca at E6 shows SOX10$^+$ ENCCs throughout the mesenchyme, with some co-expression of EdU, consistent with proliferating ENCCs. (A′,A″) The wavefront was defined as the region expressing undifferentiated SOX10$^+$ ENCCs, with no expression of HU (A′) or BFABP (A″). (B) The rate of ENCC proliferation was measured at multiple positions in E5-E8 intestine (n=9 guts per stage) by calculating the proportion of SOX10$^+$ cells that incorporate EdU, only counting undifferentiated ENCCs (SOX10$^+$, HU$^-$, BFABP$^-$). ep, epithelium; NoR, nerve of Remak. **P<0.01; ***P<0.001. Scale bar: 70 µm. n=9 guts per stage.

expression profiles were observed, with 559 differentially expressed genes (DEGs) upregulated and 894 DEGs downregulated in the ceca compared with the interceca (Fig. 6A, Table S1). HSCR-related genes (Gui et al., 2017; Karim et al., 2021) were highly represented in these data, with 51 of 96 genes analyzed being differentially expressed (FDR<0.05) between the ceca and interceca regions (Fig. 6B). This included upregulation of *Ret* in the interceca and upregulation of the genes encoding ligands GDNF and EDN3 in the ceca, as we previously reported (Nagy and Goldstein, 2006a). Over-representation analysis of Gene Ontology (GO) gene sets was performed and further processed to eliminate similar GO terms using the redundancy tool Revigo. These data revealed that DEGs upregulated in the ceca were associated with biological processes describing formation of the nervous system, cell migration, and digestive tract development (Fig. 6C, Table S2), consistent with the ceca having a molecular signature associated with the promotion of ENCC colonization. The biological processes 'cell-cell signaling by Wnt' and 'negative regulation of canonical Wnt signaling pathway' were identified as non-redundant processes enriched in DEGs upregulated in the ceca (Fig. 6C). These Wnt-related processes were ranked 278 and 273 by fold-enrichment scores, respectively, in the over-representation analysis (Table S2). Yet other Wnt-related biological processes show greater fold enrichment, such as 'regulation of non-canonical Wnt signaling pathway' (ranked 17) and 'canonical Wnt signaling' (ranked 177). A zero-order protein-protein interaction (PPI) network was generated to analyze direct interactions between DEGs in the ceca and interceca (Fig. 6D). Similar to the over-representation analysis, a key module associated with Wnt signaling was identified (Fig. 6D′, Table S3). The biological processes 'neurogenesis' (Fig. 6D″) and 'cell migration' (Fig. 6D‴) were both enriched in the PPI network (Table S3). These processes exhibited a strong overlap with the module of Wnt ligands

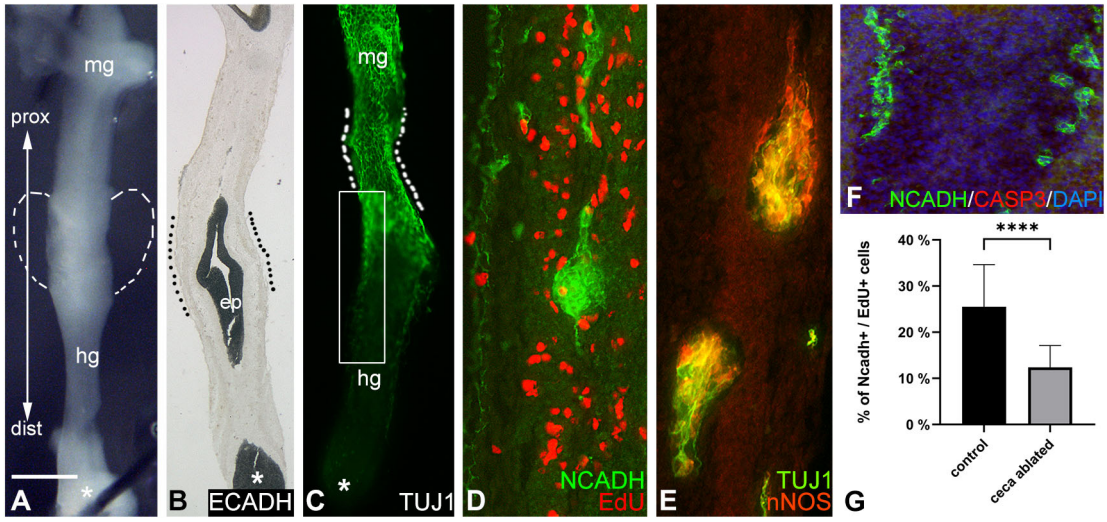

Fig. 3. Ceca are required for colonization of the hindgut ENS. (A-F) The ceca were microsurgically removed from E5 intestine (A, dashed lines demarcate where the ceca were) and the gut stained with E-cadherin (ECADH; CDH1) antibody to confirm an otherwise intact intestine (B, dotted lines mark prior location of ceca). After 72 h in organ culture, longitudinal sections were stained with TUJ1 antibody, showing ENCC migration arrested at the proximal hindgut (C, boxed area magnified in D), with formation of large NCADH$^+$ ENCC aggregates containing minimal cell proliferation (D) and extensive nNOS differentiation (E). Sections through the ceca-ablated guts were stained for cleaved caspase-3 to detect apoptosis and NCADH to label ENCCs (F). (G) Following cecal ablation, ENCC proliferation at the wavefront was significantly reduced compared with control. n=8. ****P<0.0001. dist, distal; ep, epithelium; hg, hindgut; mg, midgut; prox, proximal. Scale bar in A: 70 µm (A-C); 100 µm (D,E); 60 µm (F).

Development (2021) 148, dev199825. doi:10.1242/dev.199825

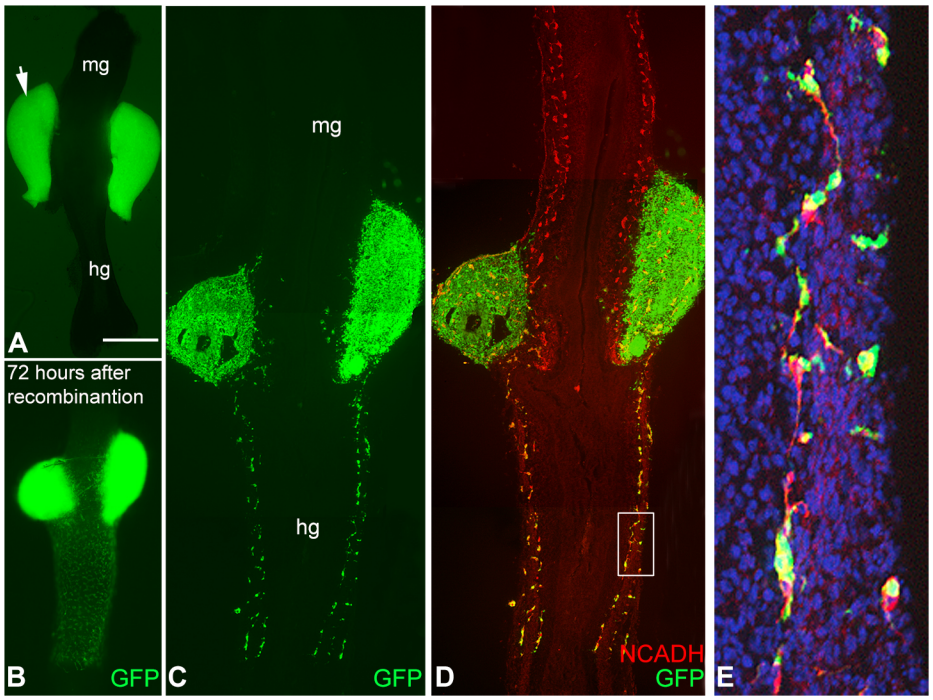

Fig. 4. Cecal chimeras reveal that the hindgut ENS arises from ceca-derived ENCCs. (A,B) After removing the ceca from E6 intestine, they were replaced by new ceca from E6 GFP$^+$ chicks (A) and the recombinants cultured for 72 h; *n*=8. (B). (C) GFP$^+$ cells migrate out of the ceca distally to populate the hindgut mesenchyme. (D,E) Co-immunofluorescence with NCADH antibody shows that the hindgut ENS arises exclusively from ceca-derived GFP$^+$ cells (boxed area magnified in E). hg, hindgut; mg, midgut. Scale bar in A: 350 µm (A,B); 200 µm (C,D); 50 µm (E).

and receptors, suggesting that Wnt pathways may be involved in these processes in the ceca. From these analyses, upregulation of key Wnt signaling ligands WNT11, WNT2B, and WNT5A, and receptors FZD4 and FZD10, were identified in the ceca. Conversely, the cognate WNT11 and WNT5A receptor, FZD7, and co-receptors RYK and PRICKLE1 of the noncanonical WNT/planar cell polarity (PCP) pathway, were identified in the intercecal region (Fig. 6E). Likewise, several modulators of WNT signaling were identified, including AMER2, DACT1 and MCC, which are antagonists of WNT/β-catenin signaling (Pfister et al., 2012); ANKRD6 and MLLT3, which suppress canonical WNT signaling and promote the PCP pathway (Haribaskar et al., 2009; Jones et al., 2014); and CTHRC1, which selectively activates WNT/PCP signaling (Yamamoto et al., 2008) (Fig. 6E).

We validated the cecal enrichment of Wnt signaling molecules, specifically WNT5A and WNT11, identified in the RNA-seq dataset and PPI network by *in situ* hybridization. *Wnt5A* and *Wnt11* were both strongly expressed in the cecal region at E5 (Fig. 7A-C). *Fzd7*, in contrast, was not expressed in the E5 ceca (Fig. 7D), although it was present in the gut epithelium at this stage (Fig. 7E). Mesenchymal expression of *Fzd7* appeared throughout the cecal and intercecal region at E6 (Fig. 7F), and could be seen in the hindgut, neural tube, dorsal root ganglia and Müllerian duct at E7.5 (Fig. 7G-I). Co-immunofluorescence with antibodies to HNK-1 (B3GAT1) and *Fzd7* in the hindgut at this stage confirmed its expression by neural crest-derived cells (Fig. 7I-J′). Interestingly, however, it was absent from the sacral neural crest-derived nerve of Remak (Fig. 7I). ENCC expression of *Fzd7* was confirmed *ex vivo* by culturing E6 ceca in the presence of GDNF to induce ENCC migration out of the explants. As shown in Fig. 7K,K′, HNK1$^+$ ENCCs co-expressed *Fzd7*, but not *Shh* (negative control; Fig. 7L,L′). Of note, in Fig. 7K′ it appears that only a subset of HNK1$^+$ ENCCs express *Fzd7*, suggesting that the ENCCs represent a heterogeneous group wherein Fzd7 expression is variable, although further studies are needed.

To examine further the role of non-canonical Wnt signaling on ENCCs as they migrate through the cecal region, E6 ceca were removed and cultured on a fibronectin-coated surface in the presence of GDNF and/or WNT11 protein (Fig. S1). In the presence of GDNF, ENCCs migrated away from the ceca and onto the fibronectin surface within 24 h (Fig. 8A,B). Extensive migration occured by 48 h (Fig. 8C), with the majority of ENCCs expressing the neuronal differentiation marker TUJ1 (Fig. 8D). This assay provides a platform for evaluating the direct effect of signaling factors on the ENCCs themselves, separate from their mesenchymal microenvironment. When GDNF was removed from the culture media after the first 24 h, migration over the next 24 h was limited and cells aggregated into large ganglion-like structures with abnormal network morphology (Fig. 8E-G) compared with when GDNF was kept in the media (Fig. 8D). However, when the media was supplemented with WNT11 after GDNF removal at 24 h, migration was restored and the abnormal cell aggregation did not occur (Fig. 8H,I). Interestingly, compared with GDNF alone (Fig. 8D), WNT11-treated cultures appeared to have many more undifferentiated ENCCs (Fig. 8I). Furthermore, WNT11 protein alone did not promote ENCC migration from the ceca (Fig. 8J-L). To analyze the effect of WNT11 on neuronal differentiation, the proportion of HNK1$^+$ ENCCs co-expressing TUJ1 was quantified in GDNF-treated cultures with or without the presence of WNT11 protein. As shown in Fig. 8M, the presence of WNT11 significantly reduced the proportion of ENCCs that underwent enteric neuronal differentiation.

To assess the effect of WNT11 on enteric neuronal differentiation in the intact gut, we examined the presence of nNOS-expressing neurons in hindgut explants. In the ENS, nNOS marks a subset of terminally differentiated enteric neurons, unlike TUJ1 or HU, which are earlier neuronal markers. E6 chick gut, including ceca and hindgut, was cultured for 3 days with or without addition of WNT11 protein. In normal media conditions, ENS colonization of the hindgut was completed and nNOS$^+$ ENCCs were present at the distal end (Fig. 9A-B′). Addition of WNT11 to the culture media did not interfere with ENCC migration (Fig. 9C), but it did inhibit neuronal differentiation, as shown by the absence of nNOS-expressing neurons in the distal hindgut (Fig. 9D,D′). This was further confirmed by

Development (2021) 148, dev199825. doi:10.1242/dev.199825

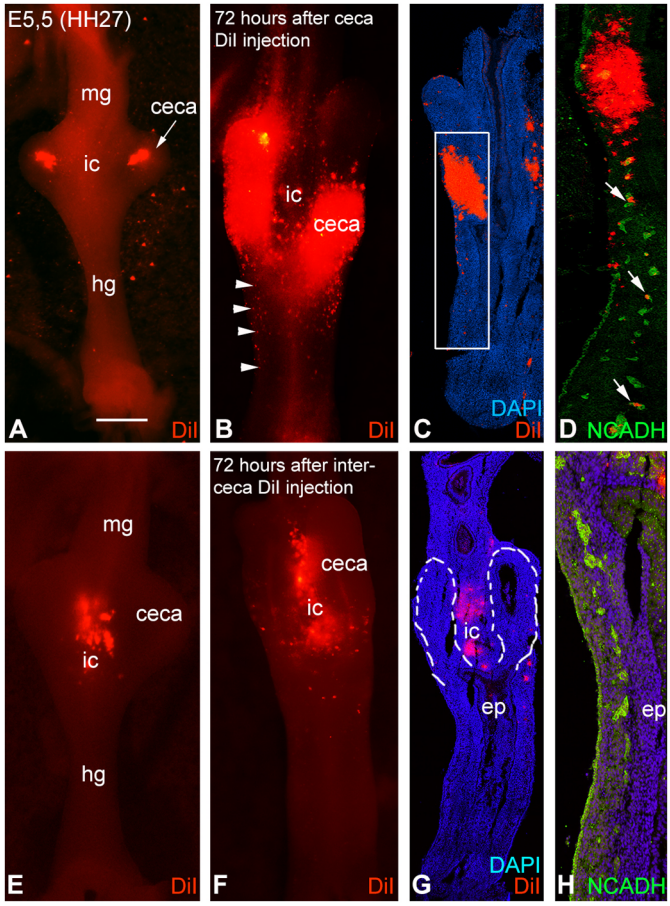

Fig. 5. Hindgut ENCCs arise from the ceca and not from the intercecal region. (A,B) Vital lipophilic red fluorescent dye (DiI) was injected into the cecal buds at E5.5 (A). After 72 h in culture (B), DiI^{+} cells are seen dispersing into the proximal hindgut on wholemount (B, arrowheads). (C,D) Longitudinal section shows DiI cells in the proximal hindgut (C), and a magnified view of the boxed area shows co-expression of NCADH, consistent with ENCCs (D, arrows). (E-H) In contrast, following DiI injection into the intercecal region (E), no DiI-labeled ENCCs are found in the hindgut (F-H; dashed lines in G denote the ceca). ep, epithelium; hg, hindgut; ic, interceca; mg, midgut. Scale bar in A: 400 µm (A,B,E,F); 300 µm (C,G); 500 µm (D,H).

measuring the distance from the distalmost NCADH^{+} cell at the distal end of the migratory wavefront to the distalmost nNOS^{+} cell. As shown in Fig. 9E, the addition of WNT11 delayed neuronal differentiation.

We examined the effect of WNT11 on ENCC proliferation. When we quantified the proportion of NCADH^{+} ENCCs that incorporated EdU in cultured E6 intestine, we found that the addition of WNT11 to the cultures reduced the rate of ENCC proliferation from 25.5±9.1% to 16.8±6.1% (mean±s.d.; P<0.001). We tested this in a second assay by culturing E6 ceca and midgut on fibronectin-coated plates for 48 h. GDNF was added to the cultures to promote ENCC migration away from the gut and onto the plates and incorporation of EdU was used to quantify cell proliferation. As shown in Fig. S2, the presence of GDNF promoted ENCC proliferation, whereas addition of WNT11 significantly reduced it.

DISCUSSION

The ENS of the foregut and midgut arises from the craniocaudal migration of vagal neural crest-derived cells within the gastrointestinal wall. Hindgut ENS development, in contrast, has several unique features. Although the majority of the ENCCs similarly come from the vagal crest, a significant proportion arise from sacral neural crest. In avians, these sacral crest-derived cells enter from the cloacal end of the gut by means of pelvic plexus and migrate cranially (Nagy et al., 2012) or they travel into the gut wall directly along nerve fibers extending from the sacral crest-derived nerve of Remak (Burns et al., 2002). Similarly, in mice, sacral neural crest cells enter through the distal end (Serbedzija et al., 1991) and, in addition, Schwann cell precursors migrate along extrinsic nerve fibers to give rise to ENCCs in the hindgut (Uesaka et al., 2015). In mice, some vagal neural crest-derived ENCCs bypass the traditional craniocaudal path to the hindgut by taking a shortcut through the intestinal mesentery that lies between the juxtaposed distal small intestine and proximal colon (Nishiyama et al., 2012). In the current study, we have identified another unique aspect of hindgut ENS formation in the avian embryo, namely the indispensable role of the ceca in development of the hindgut ENS and the observation that hindgut ENCCs arise from the cecal buds only and not from the intercecal region. We acknowledge that this was demonstrated in *ex vivo* conditions, where sacral neural crest-derived ENCCs are not present because the nerve of Remak is removed prior to organ culture. Nevertheless, our findings show that the normal craniocaudal migration of vagal crest-derived ENCCs does not simply progress as a wave through the midgut-hindgut junction. Rather, cells that migrate into the mesenchyme between the paired ceca are halted, whereas those that migrate into the cecal buds proliferate and continue their caudal migration. Furthermore, ENCC proliferation at the migratory wavefront is at its highest when the wavefront is in the cecal buds. Although ENCC proliferation has previously been shown to be high at the wavefront of migration (Barlow et al., 2008; Simpson et al., 2007), here we show that this wavefront proliferation is at its highest when the wavefront is at the cecal buds, suggesting that ENCCs receive mitogenic signals in this region to maximize their numbers in preparation for hindgut colonization.

The multiple adaptations that have developed in rodents and avians to colonize the hindgut ENS are interesting in the context of HSCR. HSCR results from incomplete colonization of the distal bowel by migrating ENCCs. Interestingly, however, the aganglionosis is limited to the colon in >90% of cases, suggesting that this distalmost end of the bowel presents a particular challenge to ENS development and that the various adaptations described above arose to circumvent that challenge. The present study suggests that abnormalities at the midgut-hindgut junction, specifically in the cecal region, may contribute to the development of HSCR. We find that when the cecal buds are experimentally removed prior to ENCC arrival, cell migration is arrested at the level of the proximal hindgut, leaving the remainder aganglionic. But rather than simply stopping their migration, they form large clusters of differentiated neurons. This suggests that signals normally present in the ceca may inhibit neuronal differentiation in order to maintain ENCCs in a progenitor state, allowing their continued migration toward the distal colorectum. This hypothesis led us to compare the transcriptomes of the cecal buds and the intercecal region at the crucial stage when the wavefront is arriving. Significant differences were identified, including upregulation in the cecal buds of genes associated with cell migration and neurogenesis. This included upregulation of *Gdnf* in the ceca, as we previously observed (Nagy and Goldstein, 2006a), and upregulation of *Ret* in the interceca. This finding is interesting as we have shown that GDNF overexpression promotes enteric neuronal differentiation and also, given the

Development (2021) 148, dev199825. doi:10.1242/dev.199825

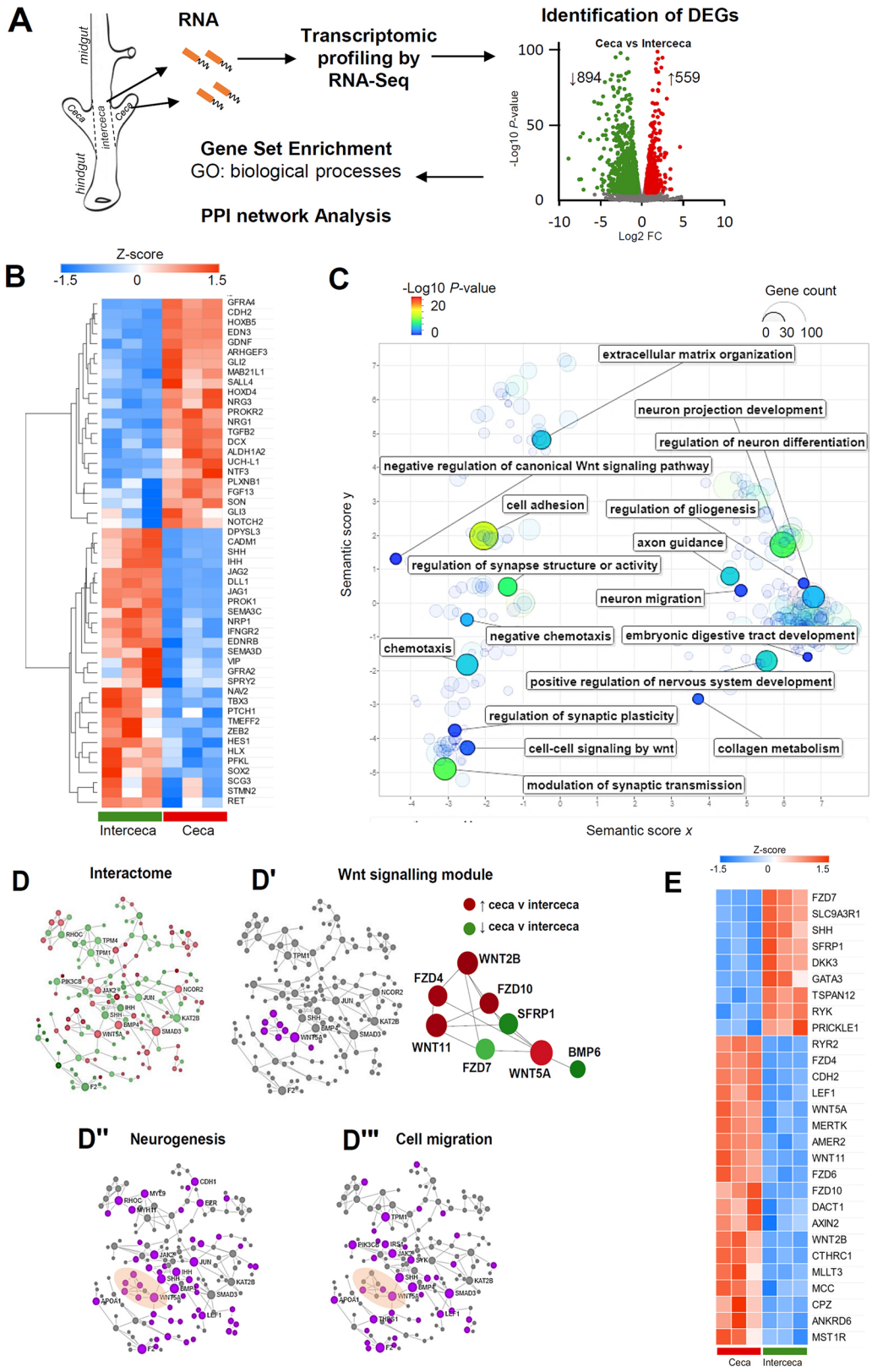

Fig. 6. See next page for legend.

chemoattractive role of GDNF to ENCCs, prevents their further migration (Mwizerwa et al., 2011), possibly accounting for our observation that ENCCs traveling through the intercecal region do not colonize the hindgut.

We noted a significant upregulation in the cecal transcriptome of Wnt signaling proteins, particularly genes encoding non-canonical Wnt proteins, including WNT11 and WNT5A. Wnt family members have diverse roles in neural crest cell migration, proliferation,

Development (2021) 148, dev199825. doi:10.1242/dev.199825

Fig. 6. Transcriptional profiling of ceca and interceca at E5. (A) Total RNA was extracted from the dissected ceca and interceca at E5 chick with RNA-seq performed to profile their respective transcriptomes. DEGs were compared between the two regions and subjected to over-representation analysis of biological processes (GO database) and protein-protein interaction network analysis. (B) Expression of HSCR-associated genes in the ceca and interceca are represented as Z-scores of RPKM values. (C) Selected biological process terms observed in genes upregulated in the ceca compared with the interceca are presented as semantic similarity scores. (D-D″) A protein-protein interaction (PPI) network of DEGs upregulated (red) and downregulated (green) in the ceca compared with the interceca was performed (D). Analysis of PPIs identified a key module associated with Wnt ligands and receptors (D′, purple dots) that were either upregulated (red) or downregulated (green) in the ceca compared with the interceca (D′, right). Overlap between Wnt signaling module (shaded) and enriched biological processes 'neurogenesis' (D″, purple dots) and 'cell migration' (D‴, purple dots) are shown. (E) Identified DEGs associated with Wnt signaling are presented as hierarchical clustered heatmaps, with data representing Z-scores of RPKM values from the cecal and intercecal regions.

differentiation and survival (Ji et al., 2019), with key roles during gut development (Theodosiou and Tabin, 2003; McBride et al., 2003). Canonical β-catenin-dependent Wnt signaling is essential for induction of neural crest cells, whereas β-catenin-independent non-canonical signaling is required for neural crest migration by directing the formation of lamellipodia and filopodia required for their delamination and migration (Carreira-Barbosa et al., 2003; Medina et al., 2000; Sumanas and Ekker, 2001; Winklbauer et al., 2001). WNT11 signaling through FZD7 has an essential role in early neural crest migration, which can be inhibited by blocking WNT11 activity and, conversely, rescued by intracellular activation of non-canonical Wnt signaling (De Calisto et al., 2005). Similarly, inhibition of ROCK1/2 kinases delays neural crest migration (Stewart et al., 2007). Marlow et al. (2002) proposed that ROCK2 acts downstream of WNT11 and is required for effective extension movements and, in melanoma, WNT11 controls invasive behavior by activating RhoA-ROCK signaling (Rodriguez-Hernandez et al., 2020).

Multiple signaling pathways have a role in ENS development in the ceca, with GDNF and EDN3 both highly and specifically expressed in this region in avians (Nagy and Goldstein, 2006a). These two pathways act in a coordinated manner to regulate ENCC migration, proliferation and differentiation as they cross the ceca. Although they both promote ENCC proliferation, EDN3 counteracts the pro-neurogenic effect of GDNF and also its chemoattractive role, thereby promoting the migration of undifferentiated progenitors into the hindgut (Nagy and Goldstein, 2006a; Mwizerwa et al., 2011). The current study adds WNT11 signaling to the mix, showing that this protein also reduces the rate of neuronal differentiation to ensure a pool of migratory progenitors for the colon. We find that WNT11 alone is not chemoattractive for ENCCs, but it is permissive, allowing the cells to respond to the pro-migratory effect of GDNF. Interestingly, in the kidney WNT11 is required for maintenance of GDNF expression (Kispert et al., 1996; Majumdar et al., 2003), which is responsible for normal ureteric branching. As WNT11 expression is directly activated by GDNF-RET signaling (Pepicelli et al., 1997), these signaling pathways may cooperate in a positive autoregulatory feedback loop, and a similar interaction may be at play in the ceca. Wnt signaling has been shown to be necessary for EDNRB-mediated proliferation and differentiation of melanocyte stem cells (Takeo et al., 2016), raising the possibility of complex interactions among all three pathways during ENS development. Our finding that WNT11 has an anti-mitogenic effect on ENCCs was surprising given the high rate of ENCC proliferation observed in the ceca, where WNT11 is expressed. How this effect is balanced with the proliferative role of GDNF and EDN3 to maintain the appropriate number of cells remains to be determined.

Our results suggest that the cecal buds in the avian intestine serve as a staging area where ENCC proliferation is promoted and differentiation is inhibited in order to maximize the number of undifferentiated progenitors available to migrate into the hindgut. Interestingly, a study in mice did not observe a higher rate of cecal ENCC proliferation (Young et al., 2005). In that study, the rate of bromodeoxyuridine-labeled ENCCs did not significantly differ in various regions of the embryonic gut, including the cecum. Given that the hindgut is the furthest distance that vagal crest-derived ENCCs need to colonize during their migration, each species may have adapted uniquely to the demands this creates on ENS development. In avians, our results show that they leveraged the position of the cecal buds as an ideal environment in which to educate arriving ENCCs to expand, maintain a non-differentiated state, and continue their craniocaudal journey into the colorectum.

MATERIALS AND METHODS

Embryos

Fertilized White Leghorn chicken (*Gallus gallus domesticus*) eggs were obtained from commercial breeders (Prophyl-BIOVO) and maintained at 37.5°C in a humidified incubator. Transgenic GFP-expressing chicken eggs were obtained from Prof. Helen Sang, The Roslin Institute, University of Edinburgh, UK (McGrew et al., 2004). Embryos were staged according to the number of embryonic (E) days or to Hamburger and Hamilton (HH) tables (Hamburger and Hamilton, 1992). Gut stages were referenced to the chick embryo gut staging table (Southwell, 2006) and the ENS formation timetable (Nagy et al., 2012).

RNA-seq

Segments of mid/hind gut were collected from the embryonic chick on E5 (HH26). The ceca and interceca regions were dissected (n=3 embryos/group) and RNA was extracted using Trizol reagent following manufacturer's instructions. Samples were submitted to the Massachusetts General Hospital Next Generation Sequencing Core facility for mRNA library construction and high-throughput sequencing using a 50 bp single-end read protocol on the Illumina HiSeq 2500 System. Base calling was performed using HiSeq Control Software and sequencing data were generated using the Illumina bcl2fastq pipeline. Sequence reads were aligned to the *Gallus gallus* reference genome (Galgal4) using the splice-aware alignment program STAR (Dobin et al., 2013). Read summarization of the raw counts per gene was determined using the program HTSeq (Anders et al., 2015). Differential expression of transcripts between the ceca and interceca were determined using the R package edgeR (Robinson et al., 2009). DEGs were identified with a P-value of <0.001 using the Benjamini–Hochberg correction (Benjamini and Hochberg, 1995). Genes with an average of <0.3 counts per million in both groups and low changes in expression (±0.5 log fold change) were removed from further analysis. Analysis of HSCR-related genes was performed using the gene set composed by Gui et al. (2017). DEGs were analyzed for overrepresentation of biological processes according to the GO database (Ashburner et al., 2000) using PANTHER (Mi et al., 2013). Enriched GO terms were summarized and presented using the GO semantic redundancy tool Revigo (Supek et al., 2011). Data for selected enriched GO terms were presented as heatmaps using ClustVis (Metsalu and Vilo, 2015). Protein-protein interaction networks and signaling modules were identified by the web-based tool NetworkAnalyst 3.0 (Zhou et al., 2019) using the STRING functional protein association networks database. Overlay of gene ontologies onto the interactome were visualized using this tool. Only interactions with experimental evidence were included in the analysis.

Immunohistochemistry and *in situ* hybridization

Tissue samples were fixed in buffered 4% formaldehyde in PBS for 1 h, rinsed with PBS, and infiltrated with 15% sucrose/PBS overnight at 4°C.

Development (2021) 148, dev199825. doi:10.1242/dev.199825

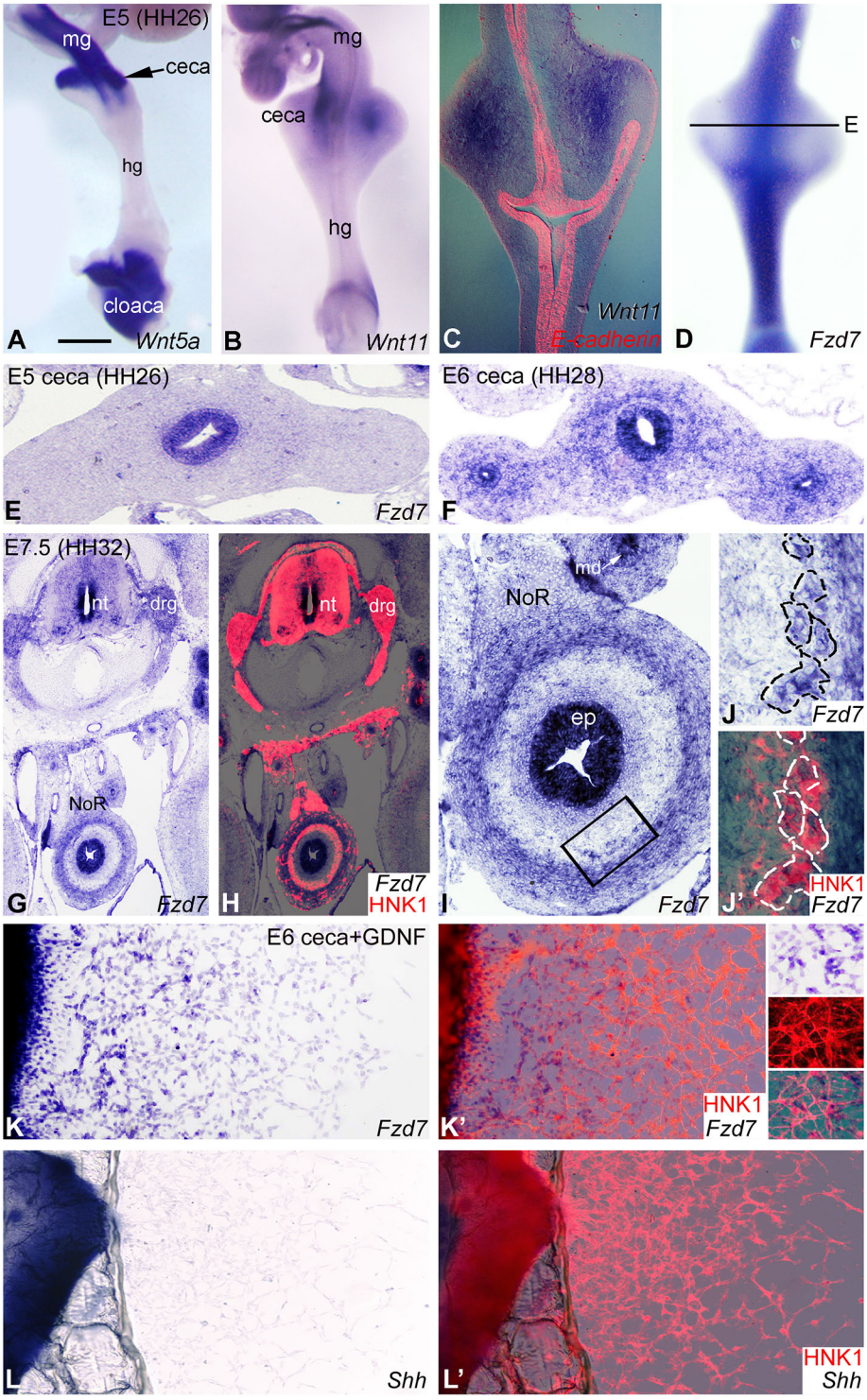

Fig. 7. Wnt pathway genes are expressed in the ceca and migrating ENCCs. (A) Whole-mount ISH of E5 distal intestine shows *Wnt5a* expressed in the midgut, ceca and cloaca. (B,C) *Wnt11* is also strongly expressed in the E5 ceca on whole-mount ISH (B) and in a longitudinal section co-stained with an E-cadherin probe to highlight the epithelium (C). (D-F) At E5, *Fzd7* is expressed throughout the gut epithelium, excluding the cecal buds (D,E) and, at E6, *Fzd7* is also expressed in the ceca and hindgut mesenchyme (F). (G-I) Cross-section through an E7.5 embryo demonstrates *Fzd7* transcript in the neural tube (nt), dorsal root ganglia (drg), Müllerian-duct (md) and hindgut. (I-J′) In the E7.5 proximal hindgut, *Fzd7* transcript is seen in the gut epithelium (I) and at the ENCC migratory wavefront (I, boxed area magnified in J,J′), but not in the nerve of Remak (I). Enteric ganglia are outlined in J,J′. (K-L′) Explanted E6 chick ceca was cultured with GDNF, which induces robust ENCC migration from the gut. *Fzd7* (K,K′), but not *Shh* (L,L′), is expressed by the migrating HNK1^{+} ENCCs. Insets show magnified view of *Fzd7*-expressing ENCCs. ep, epithelium; hg, hindgut; mg, midgut; NoR, nerve of Remak. Scale bar in A: 400 µm (A-D); 140 µm (E,F); 300 µm (G,H); 90 µm (I); 35 µm (J,J′); 100 µm (K-L′); 70 µm (insets in K′).

The medium was changed to a 7.5% gelatin, 15% sucrose mixture at 37°C for 1 h, and the tissues rapidly frozen at −50°C in methylbutane (Merck, 106056). Frozen sections were cut at 12 µm, collected on poly-L-lysine-coated slides (Sigma-Aldrich, P-8920), and stained by immunocytochemistry as previously described (Nagy and Goldstein, 2006a). Primary antibodies used were: anti-GFP (600-101-215 M, green fluorescent protein, 1:200, Rockland Immunochemicals); anti-Tuj1 (clone B1195, 1:400, Covance), a neuron-specific class III beta-tubulin; rabbit anti-neuronal nitric oxide synthase (nNOS; 1:200; Santa Cruz Biotechnology, sc-640); anti-N-cadherin (NCADH; 1:5, clone 3B6, Developmental Studies Hybridoma Bank); anti-Sox10 (1:30, clone A-2, Santa Cruz Biotechnology, sc-365692) to identify the ENCCs; and anti-E-cadherin (ECADH; 1:200, clone 36, BD Biosciences, 610181). To detect apoptosis, sections were examined with anti-activated caspase-3 (1:50, Cell Signaling Technology, 9064). After primary antibody incubation, sections were incubated with Alexa-conjugated fluorescent secondary antibodies: Alexa Fluor 488 goat anti-mouse IgG (A-32723, 1:200), Alexa Fluor 594 goat anti-mouse IgG (A-32742, 1:200), Alexa Fluor 546 goat anti-mouse IgM (A-21045, 1:200), all from Thermo Fisher Scientific (1:200). Whole-mount images were recorded with a Nikon SMZ25 fluorescence stereomicroscope, and whole-mount and section images were recorded with an Olympus IX70 fluorescence microscope. Image processing was carried out using Nikon and Olympus proprietary software,

Development (2021) 148, dev199825. doi:10.1242/dev.199825

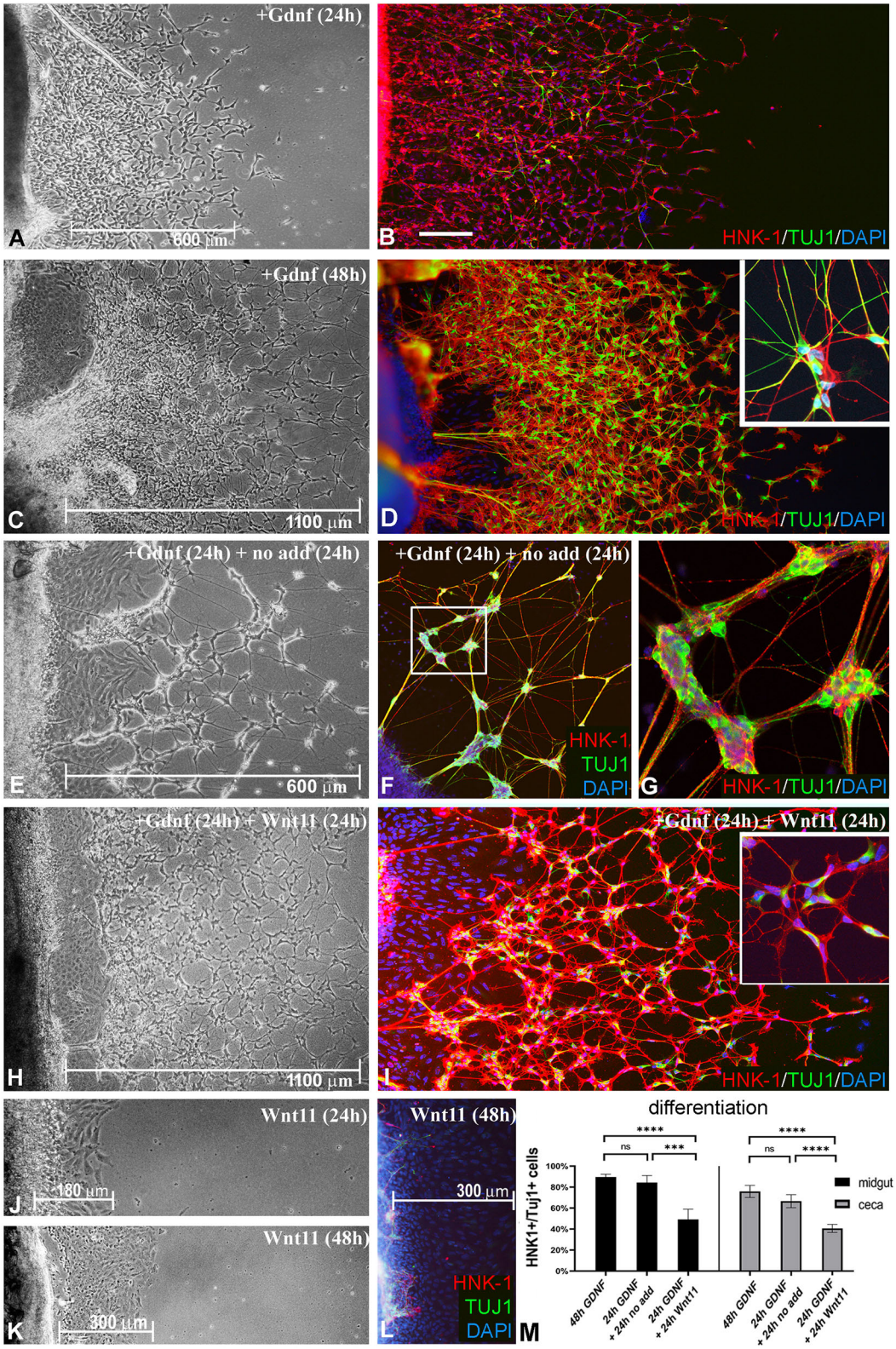

Fig. 8. WNT11 inhibits enteric neuronal differentiation. (A-D) E6 ceca were cultured on fibronectin-coated plates with GDNF for 24 h (A) or 48 h (C) and stained with HNK1 and TUJ1 antibodies (B,D) to assess ENCC migration distance and neuronal differentiation. Magnified view in inset demonstrates the neuronal differentiation. (E-I) Cultures were repeated with removal of GDNF after the first 24 h, followed by 24 h with either no added factors (E-G) or addition of WNT11 protein (H,I). Inset in I shows a magnified view of the undifferentiated ENCCs. (J-L) E6 ceca were also cultured with WNT11 protein alone for 24 h (J) or 48 h (K,L), with no ENCC migration observed. (M) The addition of WNT11 significantly inhibited neuronal differentiation of ENCCs. *n*=7-10 cell cultures/experiment. ***P<0.001, ****P<0.0001. ns, not significant. Scale bar in B: 110 µm (B,F); 135 µm (D); 70 µm (G); 125 µm (I); 35 µm (inset in I).

Development (2021) 148, dev199825. doi:10.1242/dev.199825

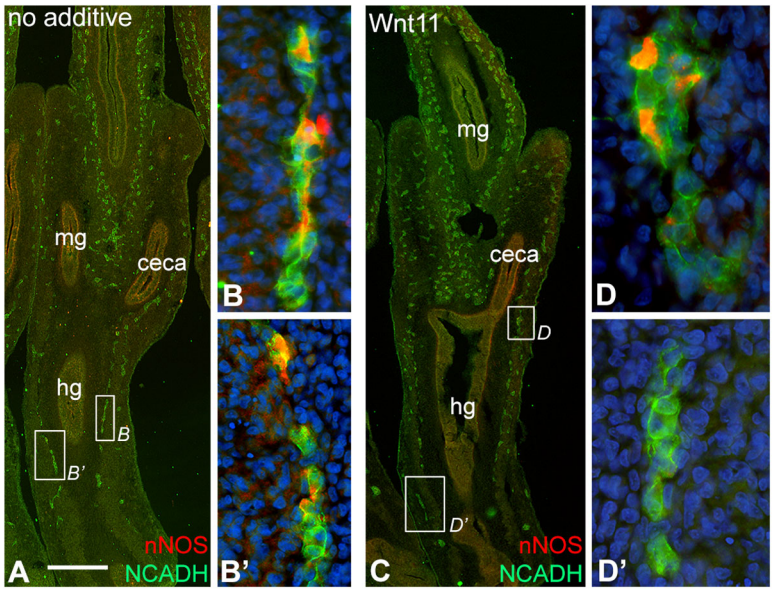

Fig. 9. WNT11 inhibits neuronal differentiation in the hindgut ENS. (A) After culturing E6 chick gut for 3 days, the hindgut ENS is fully colonized by N-cadherin$^+$ ENCCs. Boxed areas in A and C are magnified in B,B′ and D,D′. (B,B′) N-cadherin/nNOS double-immunoreactive cells are present throughout the hindgut. (C-E) When WNT11 protein is added to the culture media, N-cadherin$^+$ cells still colonize the entire hindgut (C), but nNOS immunoreactivity is present only at the proximal end (D,D′). This was quantified by measuring the distance from the distalmost NCADH$^+$ cell at the wavefront to the distalmost nNOS$^+$ cell, confirming that WNT11 delays neuronal differentiation (E). n=9. ***P<0.001. hg, hindgut; mg, midgut. Scale bar in A: 250 µm (A,C); 40 µm (B,B′); 30 µm (D,D′).

QCapture Pro and ImageJ. Image processing, including tiling and merging of pseudocolored immunofluorescence images were compiled using Adobe Photoshop 7.0.

For cell proliferation, 10 µM 5-ethynyl-20-deoxyuridine (EdU; Thermo Fisher) was added to culture medium 3 h prior to 4% paraformaldehyde (PFA) fixation. EdU incorporation was detected using the Click-iT EdU Imaging Kit (Thermo Fisher; C10337). Cell nuclei were counterstained with DAPI (4′,6-diamidino-2-phenylindole dihydrochloride; Thermo Fisher Scientific). To quantify the percentage of proliferating ENCCs, EdU$^+$ was determined at several developmental stages. Statistical analysis was performed by Kruskal–Wallis test with a post-hoc Dunn's test (R Core Team). The P-value was adjusted with Holm correction. P<0.05 was considered significant and the following further levels of significance were used: **P<0.01; ***P<0.001; ****P<0.0001. Error bars represent standard error of the mean.

In situ hybridization was performed using digoxigenin-labeled riboprobes generated from chick *Wnt5a* (Dealy et al., 1993), *Wnt11* (Marcelle et al., 1997) and *Fzd7* (Chapman et al., 2004). Riboprobe synthesis and *in situ* hybridization were performed according to standard protocols (Acloque et al., 2008).

Ceca recombination chimeras

For ceca recombination experiments, ceca buds from E6 (HH 28) GFP-chick and non-GFP chick embryonic gut was separated from the midgut-hindgut segment using Moria Pascheff-Wolff Spring scissors (Fine Science Tools). The ceca buds of the non-GFP chick embryo were replaced with ceca isolated from GFP-chick embryo. The proximal-distal and left-right orientations of the ceca buds were maintained in the recombination. To allow the tissues to adhere, ceca+intestine recombinations were embedded in a three-dimensional collagen gel matrix (BD Biosciences; 354236) as described (Nagy et al., 2007). After 3 days, recombinants were removed and immunofluorescence performed. A total of eight chimeric experiments were performed.

Intestinal organ culture assay

Guts were removed from E5 (HH26) chick embryos, pinned down to silicone-coated tissue culture plates with insect pins as described recently (Nagy et al., 2016), and allowed to float in DMEM (Sigma-Aldrich, D5429) cell culture media containing 500 ng/ml of WNT11 protein (R&D Systems, 6179-WN-010; n=28). After 3 days of culture, guts were fixed in 4% PFA and processed for immunohistochemistry.

Cell migration assay

For ENCC migration assays, distal midgut with ceca was removed from E6 (HH29) chick embryos and cultured on 20 µg/ml fibronectin-coated dishes with GDNF (10 ng/ml; R&D Systems, 212-GD-010; n=12) and WNT11 (500 ng/ml; R&D Systems; n=24) as described previously (Nagy et al., 2018).

Vital dye labeling

The vital lipophilic dye CellTracker CM-DiI (1,1′-dioctadecyl-3,3,3′,3′-tetramethylindocarbocyanine perchlorate; Thermo Fisher Scientific, C7000) was dissolved in DMSO at a concentration of 1 mg/ml. The concentrated stock DiI solution was diluted 1:100 in 15% sucrose containing PBS as described before (Nagy and Goldstein, 2006b). To study the colonization of ceca-derived or interceca-derived ENCCs in the hindgut, intestinal tracts dissected from E5.5 (HH27) chick embryos were injected with approximately 0.5 µl DiI into the ceca buds (n=9) and interceca mesenchyme (n=7). DiI-injected guts were cultured for 72 h, fixed in 4% PFA, cryoembedded in gelatin, and sectioned at 12 µm. Sections were viewed unstained with a Nikon SMZ25 epifluorescence stereomicroscope under brightfield illumination and further processed for N-cadherin immunofluorescence.

Competing interests

The authors declare no competing or financial interests.

Author contributions

Conceptualization: N.N., A.M.G.; Methodology: N.N., T.K., R.S., V.H., A.S., E.S., R.H., H.G.; Software: T.K., R.S.; Validation: N.N., T.K.; Formal analysis: T.K., R.S., V.H., A.S., E.S., R.H., H.G., A.M.G.; Investigation: N.N., T.K., R.S., V.H., H.G., A.M.G.; Resources: N.N., A.M.G.; Data curation: N.N., T.K., R.S., A.S.; Writing - original draft: N.N., A.M.G.; Writing - review & editing: N.N., A.M.G.; Visualization: T.K., R.S., V.H.; Supervision: N.N., A.M.G.; Project administration: N.N.; Funding acquisition: N.N., A.M.G.

Funding

A.M.G. is supported by the National Institutes of Health (R01DK103785). N.N. is supported a Bolyai Fellowship from the Magyar Tudományos Akadémia (Hungarian Academy of Sciences), the Excellence Program for Higher Education of Hungary from the National Research, Development and Innovation Office (FIKP-2018), and Hungarian Science Foundation NKFI grant programme (124740, 138664). Deposited in PMC for release after 12 months.

Data availability

RNA-seq data have been deposited in the Gene Expression Omnibus database under accession number GSE182783.

Peer review history

The peer review history is available online at https://journals.biologists.com/dev/article-lookup/doi/10.1242/dev.199825.

References

Acloque, H., Wilkinson, D. G. and Nieto, M. A. (2008). *In situ* hybridization analysis of chick embryos in whole-mount and tissue sections. *Methods Cell Biol.* **87**, 169-185.

Allan, I. J. and Newgreen, D. F. (1980). The origin and differentiation of enteric neurons of the intestine of the fowl embryo. *Am. J. Anat.* **157**, 137-154.

Amiel, J., Sproat-Emison, E., Garcia-Barcelo, M., Lantieri, F., Burzynski, G., Borrego, S., Pelet, A., Arnold, S., Miao, X., Griseri, P. et al. (2008). Hirschsprung disease, associated syndromes and genetics: a review. *J. Med. Genet.* **45**, 1-14.

Anders, S., Pyl, P. T. and Huber, W. (2015). HTSeq –a Python framework to work with high-throughput sequencing data. *Bioinformatics (Oxford, England)* **31**, 166-169. doi:10.1093/bioinformatics/btu638

Ashburner, M., Ball, C. A., Blake, J. A., Botstein, D., Butler, H., Cherry, J. M., Davis, A. P., Dolinski, K., Dwight, S. S. and Eppig, J. T. (2000). Gene Ontology: tool for the unification of biology. *Nat. Genet.* **25**, 25-29.

Barlow, A. J., Wallace, A. S., Thapar, N. and Burns, A. J. (2008). Critical numbers of neural crest cells are required in the pathways from the neural tube to the foregut to ensure complete enteric nervous system formation. *Development* **135**, 1681-1691. doi:10.1242/dev.017418

Benjamini, Y. and Hochberg, Y. (1995). Controlling the false discovery rate: a practical and powerful approach to multiple testing. *Journal of the Royal Statistical Society Series B (Methodological)* **57**, 289-300. doi:10.1111/j.2517-6161.1995.tb02031.x

Burns, A. J. and Le Douarin, N. M. (1998). The sacral neural crest contributes neurons and glia to the post-umbilical gut: spatiotemporal analysis of the development of the enteric nervous system. *Development* **125**, 4335-4347.

Burns, A. J., Delalande, J. M. and Le Douarin, N. M. (2002). *In ovo* transplantation of enteric nervous system precursors from vagal to sacral neural crest results in extensive hindgut colonisation. *Development* **129**, 2785-2796.

Carreira-Barbosa, F., Concha, M. L., Takeuchi, M., Ueno, N., Wilson, S. W. and Tada, M. (2003). Prickle 1 regulates cell movements during gastrulation and neuronal migration in zebrafish. *Development* **130**, 4037-4046. doi:10.1242/dev.00567

Chapman, S. C., Brown, R., Lees, L., Schoenwolf, G. C. and Lumsden, A. (2004). Expression analysis of chick Wnt and frizzled genes and selected inhibitors in early chick patterning. *Dev. Dyn.* **229**, 668-676. doi:10.1002/dvdy.10491

Dealy, C. N., Roth, A., Ferrari, D., Brown, A. M. and Kosher, R. A. (1993). Wnt-5a and Wnt-7*a* are expressed in the developing chick limb bud in a manner suggesting roles in pattern formation along the proximodistal and dorsoventral axes. *Mech. Dev.* **43**, 175-186. doi:10.1016/0925-4773(93)90034-U

De Calisto, J., Araya, C., Marchant, L., Riaz, C. F. and Mayor, R. (2005). Essential role of non-canonical Wnt signalling in neural crest migration. *Development* **132**, 2587-2597. doi:10.1242/dev.01857

Dobin, A., Davis, C. A., Schlesinger, F., Drenkow, J., Zaleski, C., Jha, S., Batut, P., Chaisson, M. and Gingeras, T. R. (2013). STAR: ultrafast universal RNA-seq aligner. *Bioinformatics* **29**, 15-21.

Druckenbrod, N. R. and Epstein, M. L. (2005). The pattern of neural crest advance in the cecum and colon. *Dev. Biol.* **287**, 125-133. doi:10.1016/j.ydbio.2005.08.040

Goldstein, A. M., Thapar, N., Karunaratne, T. B. and De Giorgio, R. (2016). Clinical aspects of neurointestinal disease: Pathophysiology, diagnosis, and treatment. *Dev. Biol.* **417**, 217-228. doi:10.1016/j.ydbio.2016.03.032

Gui, H., Schriemer, D., Cheng, W. W., Chauhan, R. K., Antiñolo, G., Berrios, C., Bleda, M., Brooks, A. S., Brouwer, R. W., Burns, A. J. et al. (2017). Whole exome sequencing coupled with unbiased functional analysis reveals new Hirschsprung disease genes. *Genome Biology* **18**, 1-13. doi:10.1186/s13059-016-1139-1

Hamburger, V. and Hamilton, H. L. (1992). A series of normal stages in the development of the chick embryo. *Dev. Dyn.* **195**, 231-272. doi:10.1002/aja.1001950404

Haribaskar, R., Putz, M., Schupp, B., Skouloudaki, K., Bietenbeck, A., Walz, G. and Schafer, T. (2009). The planar cell polarity (PCP) protein Diversin translocates to the nucleus to interact with the transcription factor AF9. *Biochem. Biophys. Res. Commun.* **387**, 212-217. doi:10.1016/j.bbrc.2009.07.012

Ji, Y., Hao, H., Reynolds, K., McMahon, M. and Zhou, C. J. (2019). Wnt signaling in neural crest ontogenesis and oncogenesis. *Cells* **8**, 1173. doi:10.3390/cells8101173

Jones, C., Qian, D., Kim, S. M., Li, S., Ren, D., Knapp, L., Sprinzak, D., Avraham, K. B., Matsuzaki, F., Chi, F. et al. (2014). Ankrd6 is a mammalian functional homolog of Drosophila planar cell polarity gene diego and regulates coordinated cellular orientation in the mouse inner ear. *Dev. Biol.* **395**, 62-72. doi:10.1016/j.ydbio.2014.08.029

Karim, A., Tang, C. S. and Tam, P. K. (2021). The emerging genetic landscape of Hirschsprung disease and its potential clinical applications. *Frontiers in Pediatrics* **9**, 638093. doi:10.3389/fped.2021.638093

Kispert, A., Vainio, S., Shen, L., Rowitch, D. H. and McMahon, A. P. (1996). Proteoglycans are required for maintenance of Wnt-11 expression in the ureter tips. *Development* **122**, 3627-3637. doi:10.1242/dev.122.11.3627

Kruger, G. M., Mosher, J. T., Tsai, Y. H., Yeager, K. J., Iwashita, T., Gariepy, C. E. and Morrison, S. J. (2003). Temporally distinct requirements for endothelin receptor B in the generation and migration of gut neural crest stem cells. *Neuron* **40**, 917-929. doi:10.1016/S0896-6273(03)00727-X

Le Douarin, N. M. and Teillet, M. A. (1973). The migration of neural crest cells to the wall of the digestive tract in avian embryo. *J. Embryol. Exp. Morphol.* **30**, 31-48.

Lee, H. O., Levorse, J. M. and Shin, M. K. (2003). The endothelin receptor-B is required for the migration of neural crest-derived melanocyte and enteric neuron precursors. *Dev. Biol.* **259**, 162-175. doi:10.1016/S0012-1606(03)00160-X

Leibl, M. A., Ota, T., Woodward, M. N., Kenny, S. E., Lloyd, D. A., Vaillant, C. R. and Edgar, D. H. (1999). Expression of endothelin 3 by mesenchymal cells of embryonic mouse caecum. *Gut* **44**, 246-252. doi:10.1136/gut.44.2.246

Majumdar, A., Vainio, S., Kispert, A., McMahon, J. and McMahon, A. P. (2003). Wnt11 and Ret/Gdnf pathways cooperate in regulating ureteric branching during metanephric kidney development. *Development* **130**, 3175-3185. doi:10.1242/dev.00520

Marcelle, C., Stark, M. R. and Bronner-Fraser, M. (1997). Coordinate actions of BMPs, Wnts, Shh and noggin mediate patterning of the dorsal somite. *Development* **124**, 3955-3963. doi:10.1242/dev.124.20.3955

Marlow, F., Topczewski, J., Sepich, D. and Solnica-Krezel, L. (2002). Zebrafish Rho kinase 2 acts downstream of Wnt11 to mediate cell polarity and effective convergence and extension movements. *Curr. Biol.* **12**, 876-884. doi:10.1016/S0960-9822(02)00864-3

McBride, H. J., Fatke, B. and Fraser, S. E. (2003). Wnt signaling components in the chicken intestinal tract. *Dev. Biol.* **256**, 18-33. doi:10.1016/S0012-1606(02)00118-5

McGrew, M. J., Sherman, A., Ellard, F. M., Lillico, S. G., Gilhooley, H. J., Kingsman, A. J., Mitrophanous, K. A. and Sang, H. (2004). Efficient production of germline transgenic chickens using lentiviral vectors. *EMBO Rep.* **5**, 728-733. doi:10.1038/sj.embor.7400171

Medina, A., Reintsch, W. and Steinbeisser, H. (2000). Xenopus frizzled 7 can act in canonical and non-canonical Wnt signaling pathways: implications on early patterning and morphogenesis. *Mech. Dev.* **92**, 227-237. doi:10.1016/S0925-4773(00)00240-9

Metsalu, T. and Vilo, J. (2015). ClustVis: a web tool for visualizing clustering of multivariate data using Principal Component Analysis and heatmap. *Nucleic Acids Res.* **43**, W566-W570. doi:10.1093/nar/gkv468

Mi, H., Muruganujan, A., Casagrande, J. T. and Thomas, P. D. (2013). Large-scale gene function analysis with the PANTHER classification system. *Nat. Protoc.* **8**, 1551.

Mwizerwa, O., Das, P., Nagy, N., Akbareian, S. E., Mably, J. D. and Goldstein, A. M. (2011). Gdnf is mitogenic, neurotrophic, and chemoattractive to enteric neural crest cells in the embryonic colon. *Dev. Dyn.* **240**, 1402-1411. doi:10.1002/dvdy.22630

Nagy, N. and Goldstein, A. M. (2006a). Endothelin-3 regulates neural crest cell proliferation and differentiation in the hindgut enteric nervous system. *Dev. Biol.* **293**, 203-217. doi:10.1016/j.ydbio.2006.01.032

Nagy, N. and Goldstein, A. M. (2006b). Intestinal coelomic transplants: a novel method for studying enteric nervous system development. *Cell Tissue Res.* **326**, 43-55. doi:10.1007/s00441-006-0207-3

Nagy, N. and Goldstein, A. M. (2017). Enteric nervous system development: A crest cell's journey from neural tube to colon. *Semin. Cell Dev. Biol.* **66**, 94-106. doi:10.1016/j.semcdb.2017.01.006

Nagy, N., Brewer, K. C., Mwizerwa, O. and Goldstein, A. M. (2007). Pelvic plexus contributes ganglion cells to the hindgut enteric nervous system. *Dev. Dyn.* **236**, 73-83. doi:10.1002/dvdy.20933

Nagy, N., Burns, A. J. and Goldstein, A. M. (2012). Immunophenotypic characterization of enteric neural crest cells in the developing avian colorectum. *Dev. Dyn.* **241**, 842-851. doi:10.1002/dvdy.23767

Nagy, N., Barad, C., Graham, H. K., Hotta, R., Cheng, L. S., Fejszak, N. and Goldstein, A. M. (2016). Sonic hedgehog controls enteric nervous system development by patterning the extracellular matrix. *Development* **143**, 264-275.

Nagy, N., Barad, C., Hotta, R., Bhave, S., Arciero, E., Dora, D. and Goldstein, A. M. (2018). Collagen 18 and agrin are secreted by neural crest cells to remodel their microenvironment and regulate their migration during enteric nervous system development. *Development* **145**, ev160317. doi:10.1242/dev.160317

Nishiyama, C., Uesaka, T., Manabe, T., Yonekura, Y., Nagasawa, T., Newgreen, D. F., Young, H. M. and Enomoto, H. (2012). Trans-mesenteric neural crest cells are the principal source of the colonic enteric nervous system. *Nat. Neurosci.* **15**, 1211-1218. doi:10.1038/nn.3184

Pepicelli, C. V., Kispert, A., Rowitch, D. H. and McMahon, A. P. (1997). GDNF induces branching and increased cell proliferation in the ureter of the mouse. *Dev. Biol.* **192**, 193-198. doi:10.1006/dbio.1997.8745

Pfister, A. S., Tanneberger, K., Schambony, A. and Behrens, J. (2012). Amer2 protein is a novel negative regulator of Wnt/beta-catenin signaling involved in neuroectodermal patterning. *J. Biol. Chem.* **287**, 1734-1741. doi:10.1074/jbc.M111.308650

Robinson, M. D., McCarthy, D. J. and Smyth, G. K. (2009). edgeR: a Bioconductor package for differential expression analysis of digital gene expression data. *Bioinformatics* **26**, 139-140. doi:10.1093/bioinformatics/btp616

Rodriguez-Hernandez, I., Maiques, O., Kohlhammer, L., Cantelli, G., Perdrix-Rosell, A., Monger, J., Fanshawe, B., Bridgeman, V. L., Karagiannis, S. N., Penin, R. M. et al. (2020). WNT11-FZD7-DAAM1 signalling supports tumour initiating abilities and melanoma amoeboid invasion. *Nat. Commun.* **11**, 5315. doi:10.1038/s41467-020-18951-2

Serbedzija, G. N., Burgan, S., Fraser, S. E. and Bronner-Fraser, M. (1991). Vital dye labelling demonstrates a sacral neural crest contribution to the enteric nervous system of chick and mouse embryos. *Development* **111**, 857-866. doi:10.1242/dev.111.4.857

Shin, M. K., Levorse, J. M., Ingram, R. S. and Tilghman, S. M. (1999). The temporal requirement for endothelin receptor-B signalling during neural crest development. *Nature.* **402**, 496-501. doi:10.1038/990040

Simpson, M. J., Zhang, D. C., Mariani, M., Landman, K. A. and Newgreen, D. F. (2007). Cell proliferation drives neural crest cell invasion of the intestine. *Dev. Biol.* **302**, 553-568. doi:10.1016/j.ydbio.2006.10.017

Southwell, B. R. (2006). Staging of intestinal development in the chick embryo. *Anat. Rec. A. Discov. Mol. Cell. Evol. Biol.* **288A**, 909-920. doi:10.1002/ar.a.20349

Stewart, A. L., Young, H. M., Popoff, M. and Anderson, R. B. (2007). Effects of pharmacological inhibition of small GTPases on axon extension and migration of enteric neural crest-derived cells. *Dev. Biol.* **307**, 92-104.

Sumanas, S. and Ekker, S. C. (2001). Xenopus frizzled-7 morphant displays defects in dorsoventral patterning and convergent extension movements during gastrulation. *Genesis* **30**, 119-122. doi:10.1002/gene.1044

Supek, F., Bošnjak, M., Škunca, N. and Šmuc, T. (2011). REVIGO summarizes and visualizes long lists of gene ontology terms. *PLOS ONE* **6**, e21800. doi:10.1371/journal.pone.0021800

Takeo, M., Lee, W., Rabbani, P., Sun, Q., Hu, H., Lim, C. H., Manga, P. and Ito, M. (2016). EdnrB governs regenerative response of melanocyte stem cells by crosstalk with Wnt signaling. *Cell Reports* **15**, 1291-1302.

Theodosiou, N. A. and Tabin, C. J. (2003). Wnt signaling during development of the gastrointestinal tract. *Dev. Biol.* **259**, 258-271. doi:10.1016/S0012-1606(03)00185-4

Uesaka, T., Nagashimada, M. and Enomoto, H. (2015). Neuronal differentiation in Schwann cell lineage underlies postnatal neurogenesis in the enteric nervous system. *J. Neurosci.* **35**, 9879-9888. doi:10.1523/JNEUROSCI.1239-15.2015

Winklbauer, R., Medina, A., Swain, R. K. and Steinbeisser, H. (2001). Frizzled-7 signalling controls tissue separation during Xenopus gastrulation. *Nature.* **413**, 856-860. doi:10.1038/35101621

Woodward, M. N., Sidebotham, E. L., Connell, M. G., Kenny, S. E., Vaillant, C. R., Lloyd, D. A. and Edgar, D. H. (2003). Analysis of the effects of endothelin-3 on the development of neural crest cells in the embryonic mouse gut. *J. Pediatr. Surg.* **38**, 1322-1328. doi:10.1016/S0022-3468(03)00389-0

Yamamoto, S., Nishimura, O., Misaki, K., Nishita, M., Minami, Y., Yonemura, S., Tarui, H. and Sasaki, H. (2008). Cthrc1 selectively activates the planar cell polarity pathway of Wnt signaling by stabilizing the Wnt-receptor complex. *Dev. Cell.* **15**, 23-36. doi:10.1016/j.devcel.2008.05.007

Young, H. M., Hearn, C. J., Farlie, P. G., Canty, A. J., Thomas, P. Q. and Newgreen, D. F. (2001). GDNF is a chemoattractant for enteric neural cells. *Dev. Biol.* **229**, 503-516.

Young, H. M., Turner, K. N. and Bergner, A. J. (2005). The location and phenotype of proliferating neural-crest-derived cells in the developing mouse gut. *Cell Tissue Res.* **320**, 1-9. doi:10.1007/s00441-004-1057-5

Yntema, C. L. and Hammond, W. S. (1954). The origin of intrinsic ganglia of trunk viscera from vagal neural crest in the chick embryo. *J. Comp. Neurol.* **101**, 515-541.

Zhou, G., Soufan, O., Ewald, J., Hancock, R. E. W., Basu, N. and Xia, J. (2019). NetworkAnalyst 3.0: a visual analytics platform for comprehensive gene expression profiling and meta-analysis. *Nucleic Acids Res.* **47**, W234-W241. doi:10.1093/nar/gkz240